Merino, M; Ahedo, E. Influence of electron and ion thermodynamics on the magnetic nozzle plasma expansion, *in* IEEE transactions on plasma science, Special issue: 33rd International Electric Propulsion Conference, IEPC 2013, October 6 to 10, 2013 Washington, D.C., Vol. 43, issue 1, Jan. 2015, Pp. 244-251
DOI: https://doi.org/10.1109/TPS.2014.2316020

Influence of Electron and Ion Thermodynamics on the Magnetic Nozzle Plasma Expansion

Mario Merino and Eduardo Ahedo

***Abstract*—A two-fluid, two-dimensional model of the supersonic plasma flow in a propulsive magnetic nozzle is extended to include simple electron and ion thermodynamics to study the effects of electron cooling and ion thermal energy on the expansion. A faster electron cooling rate is seen to reduce plasma jet divergence, increase radial rarefaction, and enhance detachment from the closed magnetic lines. Ion thermal energy is converted to directed kinetic energy by the MN without the mediation of an ambipolar electric field, and alters the electric response of the plasma.**

I. Introduction

A magnetic nozzle (MN) is an applied convergent-divergent magnetic field capable of guiding the expansion of an energetic plasma jet and accelerating it supersonically into vacuum. The *contactless* operation of MNs reduces or avoids the detrimental durability and efficiency issues associated to plasma-wall interactions, and provides superior control over the expansion. These qualities make them an interesting device to produce thrust in space. Currently, several advanced plasma thrusters, including the Helicon Plasma Thruster[1], [2], [3] (HPT), the Electron Cyclotron Resonance Thruster[4] (ECRT), the Applied-Field MagnetoPlasmaDynamic thruster[5], [6], [7] (AF-MPD), and the VASIMR[8], employ a MN as their main acceleration stage.

In a MN, the internal energy of the plasma is transformed into directed kinetic energy, much like in the case of a neutral gas in a traditional, solid de Laval nozzle. Therefore, all plasma thrusters operating on a MN are, in essence, thermal rockets: this means that specific impulse is roughly proportional to the square root of the temperature to which the plasma is heated inside the plasma source over the ion mass, i.e., $I_{sp} \propto \sqrt{T/m_i}$, requiring very large temperatures (tens to hundreds of eV) to achieve competitive I_{sp} with usual propellants like Argon or Xenon. Notwithstanding, MNs (and the plasma thrusters relying on them) constitute an attractive propulsive technology thanks to their higher thrust-to-power ratio, simplicity, robustness, versatility, and presumed long useful life. As an example, consider the HPT, which consists merely of a quartz tube wrapped by a helicon antenna, into which the propellant is injected; a RF power source to feed the antenna, ionize and energize the plasma; and solenoids or permanent magnets that create the necessary magnetic field inside and outside the tube[9]. The HPT can in principle be fed with multiple gases; and has no naked electrodes (which are the critical life-limiting element in traditional plasma thrusters). Additionally, MNs bring up the interesting possibility of enhanced 'throttleability' (the ability to adapt the specific impulse and thrust of the device in-flight by modifying the massflow, applied power, and the intensity and geometry of the magnetic field).

In contrast to a solid nozzle, which has a physical wall on where the propellant exerts a pressure force to produce thrust, the more complex physics of a plasma flowing in a MN give rise to a variety of *acceleration mechanisms*, not present in a solid nozzle, which involve[10] (*i*) azimuthal, diamagnetic electric currents in the plasma and the magnetic force on them, (*ii*) the development of an ambipolar electric field that transforms electron energy into ion energy, (*iii*) the possible formation of electric double layers within the plasma flow, and (*iv*) the long-range interaction via the plasma-induced magnetic field. Interestingly, all these aspects depend strongly on the form in which the internal energy is stored in the plasma (i.e., the particularities of the energy distribution function of each species), and how this energy evolves downstream. Another distinctive feature of MNs is the closed nature of the magnetic lines, in contrast to the finite length of a solid nozzle. This raises the question of efficient plasma detachment[11] from the magnetic field to form a free plume downstream (an issue not present in ground applications of MNs such as advanced plasma treatments of material surfaces). Without proper detachment, the plasma would instead turn back along the magnetic streamlines, ruining thrust and endangering the spacecraft.

Current understanding of MN physical phenomena is due to a limited number of experiments, normally linked to particular plasma thruster prototypes, and models of the plasma flow in the magnetic field. As relevant examples, the experiments of Andersen *et al.* [12], Kuriki *et al.* [13], York *et al.* [14] and Inutake *et al.* [15] demonstrate the basic operation of the MN, including the supersonic acceleration of the ion flow, and the existence of the ambipolar acceleration mechanism. These developments were accompanied by several theoretical developments, mainly based on simple fluid 1D models, 2D models or single-particle models, such as those of Kosmahl[16], Chubb[17], Gerwin *et al.* [11], Sercel[18] and Mikellides *et al.* [19]. Some of these models, however, rely upon two assumptions which have proven to be inadequate for the study of MNs: the use of a basic Ohm's law that ignores Hall and pressure terms completely (to first order, it is the *difference* between these two terms what governs the development of the electric field in a MN), and second, the imposition of strong current ambipolarity (that is, ions and electrons are forced

Manuscript received XXXXXX; revised XXXXXX

The authors are with Universidad Carlos III de Madrid, Av. de la Universidad 30, 28911 Leganés (Madrid), Spain (e-mail: mario.merino@uc3m.es; eduardo.ahedo@uc3m.es). More information on aero.uc3m.es/ep2

Color versions of one or more of the figures in this paper are available online at http://ieeexplore.ieee.org.

to expand identically, forbidding any internal separation of the two flows). These assumptions are avoided in Ref. [10], where we formulate a two-dimensional, two-fluid model that illustrates the main acceleration mechanisms in a hot-electron, cold-ion plasma and shows that the thrust generated by the MN is the magnetic reaction force caused by the diamagnetic plasma currents on the MN generator. The diamagnetic nature of the plasma currents was observed by Roberson *et al.* [20], and the magnetic character of thrust was later confirmed by Takahashi *et al.* [21].

In the last two decades, much of the MN-related work has focused on the study of plasma detachment. Experiments by Cox *et al.* [22], Deline *et al.* [23], Terasaka *et al.* [24], Squire *et al.* [25], and Takahashi *et al.* [26] all show that detachment begins to take place, to some extent, in the near-region (i.e., up to a few plasma radii away from the thruster exit). Notwithstanding, a successful explanation of this phenomenon remains to be found. Moses *et al.* [27], Hooper[28] and Arefiev *et al.* [29] proposed different separation mechanisms, based on different types of MHD cold-plasma models. However, the conclusions of these studies were recently shown to be inapplicable to MN expansion of hot plasmas, the case of interest for propulsion[30], [31].

Characterization of plasma detachment in the far-region (once most acceleration has taken place and magnetic lines start to turn around) has remained therefore elusive. The reason lays in the formidable difficulties involved in studying the far-region plume, both with experiments, where vacuum requirements to avoid plasma-ambient interaction are too high for laboratory tests and very large chambers are needed, and in the modeling/simulation realm, where phenomena like demagnetization, resistivity, anisotropization, thermodynamic behavior of each species, interaction with an ambient plasma or an external magnetic field, and non-neutral effects associated to the very low densities are no longer negligible and have to be considered. A first analysis[32] (which nonetheless neglects these effects) shows that the massive ions, which become non-magnetized soon after entering the divergent MN, do not follow magnetic lines but instead separate *inward* from the field, carrying the plasma momentum with them and effectively forming a free plume. The phenomenon takes place in a globally current free jet, even if electrons remain fully-magnetized and turn around with the field; only a negligible fraction of the ion flow is indeed pulled along with the electrons to maintain quasineutrality in the whole domain. This result is in agreement with the experimental observations[22], [23], [24], [26] of ion flux tube separation.

One of the determinant aspects for the far-region expansion is the rate at which electron cooling takes place. Experimental measurements[15], [23] suggest that electron temperature varies only slowly along the near-region, with an 'effective' polytropic exponent between 1 (fully isothermal model) and 1.2. Raadu[33], on the other hand, predicts an adiabatic cooling of the electrons with a 1D self-similar expansion model, acknowledging that some rethermalization process should be invoked to explain the near-constant observed temperatures. At any rate, a mechanism for collisionless electron cooling in the MN must exist downstream, likely involving potential barriers and anisotropization[34], [35], and complex heat fluxes. Additionally, anomalous electron thermodynamics could also explain certain flow structures like weak electric double layers[36], [37], [38], which have been observed in some HPT prototypes[39].

Another aspect of interest in MNs is the distinct roles of electron and ion thermal energies (or their temperatures, T_e and T_i), in the expansion. While measurements indicate that in many cases $T_i \ll T_e$, such as in HPTs or ECRTs (and to some extent AF-MPDs too), and therefore many of the existing plasma/MN models disregard ion temperature, this is not the case in other devices such as the VASIMR, where the ion-cyclotron resonance heater (ICRH) deposits most of the applied power directly into ions (~ 170 kW on the ICRH compared to ~ 30 kW deposited on the source[25]). Whereas the expansion in the former examples is driven by electron thermal energy (giving rise to the ambipolar acceleration mechanism), it is driven by ion thermal energy in the latter.

In this Paper we perform a first assessment of the effects of electron cooling and ion temperature in the plasma acceleration and plume formation. To this end, our 2D plasma/MN model[10] is extended to treat both the electrons and ions as a hot polytropic species, which can be regarded as an 'effective' cooling law. The present analysis does not inquire on the physical mechanisms responsible for electron cooling, nor on the kinetic evolution of the species (which will be object of future research). In the absence of a model of the anisotropization of the magnetized electrons or ions, in this preliminary stage we will assume that both populations remain close to Maxwellian as they expand downstream. The results are compared against the fully isothermal electron and cold ion plasma jet with zero cooling, analyzing the differences found in the behavior of plasma forces, ambipolar electric field, and overall efficiencies. The limitations of isothermal models are discussed.

The rest of the paper is structured as follows. Next Section briefly introduces the extended model with polytropic electrons and non-zero ion temperature. Electron cooling effects are investigated in Section III. The role of ion temperature is discussed in Section IV. Finally, conclusions of this analysis and an outlook into further steps to understand the thermodynamics of a plasma in a MN are presented in Section V.

II. Extended MN/plasma model

The MN/plasma thermodynamics model discussed here generalizes our cold ion, isothermal electron model, described in detail in Ref. [10]. As such, in this section only the distinctive aspects of the extended model are presented, with a brief, self-contained summary of the hypotheses and main equations to facilitate the comprehension of the rest of the paper.

The model describes the axysimmetric, supersonic expansion of a hot plasma column in a divergent magnetic field. The plasma is injected at the magnetic throat, located at $z = 0$. The plasma is assumed collisionless, quasineutral, and globally-current-free. This does not preclude, however, the formation of local longitudinal electric currents, as long as their integral over any jet section equals zero. Electrons

have negligible inertia and are fully-magnetized, meaning that electron streamtubes are magnetic streamtubes. Heavier ions, on the other hand, are allowed to have any magnetization degree. Under these assumptions, the plasma responds to following equations:

$$\nabla \cdot (n\boldsymbol{u}_i) = 0, \tag{1}$$

$$\nabla \cdot (n\boldsymbol{u}_e) = 0, \tag{2}$$

$$nm_i \left(\boldsymbol{u}_i \cdot \nabla\right) \boldsymbol{u}_i = -\nabla \cdot \mathcal{P}_i - en\nabla\phi + en\boldsymbol{u}_i \times \boldsymbol{B}, \tag{3}$$

$$0 = -\nabla \cdot \mathcal{P}_e + en\nabla\phi - enu_{\theta e}B\mathbf{1}_\perp, \tag{4}$$

where n, $\boldsymbol{u}_i$ and $\boldsymbol{u}_e$ stand for the plasma density, ion velocity, and electron velocity; $\mathcal{P}_i$ and $\mathcal{P}_e$ are the ion and electron pressure tensors; ϕ and $\boldsymbol{B}$ are the electric potential and the magnetic field; and $\mathbf{1}_\perp$ is a unit vector perpendicular to the magnetic field (so that $\left[\mathbf{1}_\parallel, \mathbf{1}_\perp, \mathbf{1}_\theta\right]$ constitutes a local orthonormal reference system). In the following, the induced magnetic field that the plasma generates is neglected, assuming a low plasma β (although it can be included easily with an iterative approach [40]), keeping only the applied magnetic field, which satisfies $r\boldsymbol{B} = \nabla\psi \times \mathbf{1}_\theta$, with ψ the magnetic streamfunction.

Equations (1)–(4) need to be closed with a thermodynamic model for $\mathcal{P}_i$ and $\mathcal{P}_e$. While the non-isotropic nature of the pressure tensors can be important (and in some devices, such as the VASIMR, it certainly is), in the present work both species are treated as isotropic and Maxwellian, i.e., $\mathcal{P}_j = p_j\mathcal{I}$, with $p_j = nT_j$, and $\mathcal{I}$ is the identity tensor (for $j = i, e$). Although limited, this approach still allows us to retain and study the effects of electron cooling and ion thermal energy on the expansion, without delving into the kinetic features of the plasma. The evolution of each species is further modeled with a polytropic law,

$$T_i = T_{i0}(n/n_0)^{\gamma_i - 1}, \tag{5}$$

$$T_e = T_{e0}(n/n_0)^{\gamma_e - 1}, \tag{6}$$

where γ_i, γ_e are 'effective' specific heat ratio exponents for ions and electrons, not necessarily equal, which reflect their cooling rates, and magnitudes with subindex '0' are evaluated at the origin, $z = r = 0$. As explained in the Introduction, γ_i, γ_e depend on several aspects of the collisionless expansion such as potential barriers, and their calculation requires modeling the plasma response at a kinetic level. Experimental measurements suggest cooling rates below the adiabatic value (5/3 for electrons and single atoms with three degrees of freedom). Macroscopically, this means the existence of plasma heat fluxes into the downstream region to maintain thermal energy levels in the plume above those of the adiabatic expansion.

The above model for ions and electrons allows to define a barotropy function for each,

$$h_i = \frac{\gamma_i}{\gamma_i - 1}T_i; \quad h_e = \frac{\gamma_e}{\gamma_e - 1}T_e \tag{7}$$

that satisfies $ndh_j = dp_j$ (for $j = i, e$). Observe that in the isothermal limit for species j ($\gamma_j = 1$), the barotropy function becomes $h_j = T_{j0}\ln(n/n_0)$.

Using these expressions, electron momentum equation projected along $\mathbf{1}_\parallel$ and $\mathbf{1}_\perp$, yields, respectively,

$$H_e(\psi) = h_e - e\phi \equiv h - e\tilde{\phi}, \tag{8}$$

$$eu_{\theta e}/r = -dH_e/d\psi, \tag{9}$$

where $H_e(\psi)$ is the tube-wise Bernoulli function, and Eq. (3) can be rewritten as

$$m_i \left(\boldsymbol{u}_i \cdot \nabla\right) \boldsymbol{u}_i = -e\nabla\tilde{\phi} + e\boldsymbol{u}_i \times \boldsymbol{B}, \tag{10}$$

where $h = h_i + h_e$ and $e\tilde{\phi} = e\phi + h_i$. Note that in the variables h, $\tilde{\phi}$, Eqs. (8) (9) and (10) become analogous to the cold ion model of Ref. [10] (except that h has a more complex expression). Hence, like in the basic model, Eqs. (8) (9) still indicate the conservation of H_e and $u_{\theta e}/r$ along magnetic/electron streamtubes.

Examination of these expressions shows that the effective ion sound velocity is given by

$$c_s^2 = \frac{\gamma_e T_e + \gamma_i T_i}{m_i}, \tag{11}$$

which can be used to define the longitudinal ion Mach number M, given by $M^2 = \left(u_{zi}^2 + u_{ri}^2\right)/c_s^2$.

As the ion flow in the divergent MN is supersonic ($M \geq 1$), the resulting model constitutes an hyperbolic problem for ions, susceptible of efficient integration with the method of characteristics. This method is applied to Eqs. (1) and (3), using Eq. (8) to provide the necessary relation between ϕ and n (through h). Parallelly or afterward, Eq. (2) yields $u_{\parallel e}$. Likewise, Eq. (9) can be used to calculate the Hall velocity $u_{\theta e}$.

A recent restructuration of the integration algorithms in the DIMAGNO code allows integrating beyond the turning point of the MN[32]. Since the effects of changing the magnetic field divergence rate and strength have been studied already elsewhere[10], in this paper the MN geometry is simply given by a single current loop located at $z = 0$, $r = 3.5R$, where R is the radius of the plasma jet at the throat, and the magnitude of the magnetic field is fixed at $eBR/\sqrt{m_i T_{e0}} = 0.1$ (ions essentially unmagnetized). The resulting MN has a turning point located at $z = z_{TP} \simeq 16R$.

III. Effects of electron cooling

To focus the discusion on the effects of electron cooling, simulations with plasma conditions $n(0, r) = n_0$, $\phi(0, r) = 0$, $u_{\theta i}(0, r) = 0$ and $T_{i0} = 0$ are used in this section, with different values of γ_e: 1.1, 1.2, 1.3 (moderate cooling rates) and 1 (isothermal electrons limit).

Equation (8) condenses the effect of electron streamline thermodynamics on the behavior of the ambipolar electric potential, ϕ, from where various aspects can be already inferred.

First, as plotted in Fig. 1, the polytropic cooling law considered here reproduces the existence of an asymptotic value of the potential. From Eq. (8),

$$e\phi \to e\phi_\infty = -\frac{\gamma_e}{\gamma_e - 1}T_{e0}, \text{ as } (n, T_e) \to 0. \tag{12}$$

A bounded potential is one of the first expected features of the MN expansion. This stands in contrast to the unphysical behavior in an isothermal model, where ϕ continues to decrease

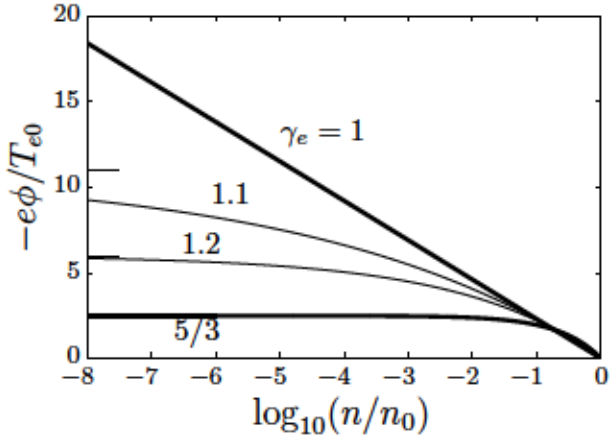

Fig. 1. Ambipolar electric potential ϕ as a function of plasma density n, for different values of γ_e. The corresponding asymptotic values $e\phi_\infty/T_{e0}$ for the polytropic cases are marked on the left side of the diagram.

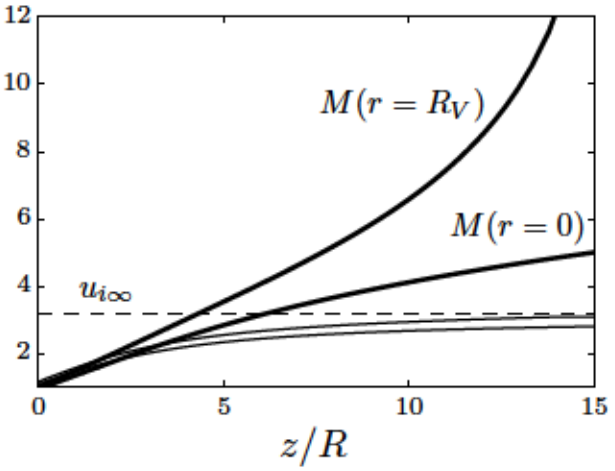

Fig. 2. Plasma Mach number (thick lines) along the MN axis ($r = 0$) and plasma edge (R_V) for $\gamma_e = 1.3$. The two unlabeled, thinner lines are the ion velocity on the axis (lower line) and the edge (upper line). The asymptotic ion velocity for a complete expansion, $u_{i\infty} = \sqrt{2\phi_\infty/m_i + u_{i0}^2}$ is shown as a dashed line. Ion velocities are non-dimensionalized with $\sqrt{T_{e0}/m_i}$.

(logarithmically) to infinity. This inconsistency of isothermal models was already by Refs. [34], [35].

Second, while $u_i \propto \sqrt{-\phi}$ is consequently upper-bounded, and it grows at a lower rate than in the isothermal limit, the rapid decrease of the sonic velocity $c_s \propto \sqrt{T_e}$ makes the ion Mach number M increase at a faster rate (Fig. 2). This behavior is more marked at the plasma edge, where the case displayed reaches $M = 12$, meaning that the plasma is already hypersonic before the turning point (the equivalent isothermal plasma, in contrast, reaches only a third of that value at that position). Ion velocity u_i is seen to approach rapidly its asymptotic value both at the axis and the edge, and the differences between the two locations are smaller than in the isothermal plasma.

The fact that the plasma becomes hypersonic sooner due to cooling means that the magnitude of pressure and electric forces (which scale as the electron pressure, Eq. (4)) decreases faster along the MN, thus affecting the development of the plume in the far region. A first consequence of this is that

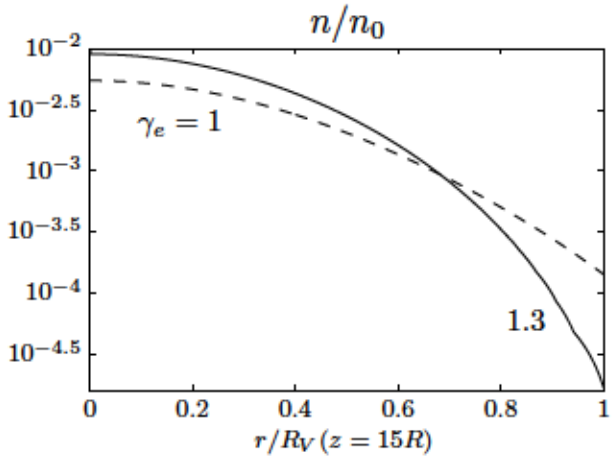

Fig. 3. Plasma density profile at $z = 15R$ (near the turning point), for the isothermal ($\gamma_e = 1$, dashed line) and polytropic ($\gamma_e = 1.3$) plasmas. $R_V(z)$ is the radius of the plasma tube at z.

ions are not pulled radially-outward as intensely as in the isothermal limit, resulting in a more collimated jet. Indeed, the density profiles are much steeper in the polytropic plasma, accentuating the already strong 2D nature of the plasma expansion. This is shown in Fig. 3, which reveals a difference in density of one order of magnitude near the turning point with respect to the isothermal limit: while density near the axis remains higher, a larger rarefaction occurs at the plasma edge.

The aforementioned faster decay of the electromagnetic forces on ions along the MN means that these forces become sooner uncapable of deflecting the direction of the ion streamtubes to match them with magnetic streamtubes. As a result, ion streamtubes separate from magnetic/electron tubes and become almost straight, carrying the plasma momentum away from the MN without being dragged back towards the thruster, even if electrons are still fully-magnetized. While this phenomenon occurs also in an isothermal plasma when ions become unmagnetized and hypersonic[32], it is more prominent under the effects of electron cooling, as can be observed in Fig. 4, where the earlier growth of ion separation results in a lower streamtube divergence angle downstream. This figure depicts the evolution of the ion streamtubes containing 10%, 50% and 95% of the ion mass flow, and their initially-matching electron/magnetic tubes. Most of the plasma mass detaches robustly from the closed magnetic lines, with the exception of a negligible fraction of the peripheral ion flow, which under the quasineutrality hypothesis of the model is forced to return along the jet edge with the electrons (less than $< 0.5\%$ in all simulations). As evidenced in Fig. 4, cooling facilitates plasma detachment as it promotes the earlier ion inward separation. Notice that this mechanism would not be observable under the hypothesis of local current ambipolarity in the plasma: ion separation is linked to the formation of local longitudinal electric currents in the globally current-free plasma jet.

Quantification of plasma detachment can be performed with the plume divergence efficiency, $\eta_{plume,95\%}(z)$. This is defined as the ratio between axial and total ion kinetic energy carried

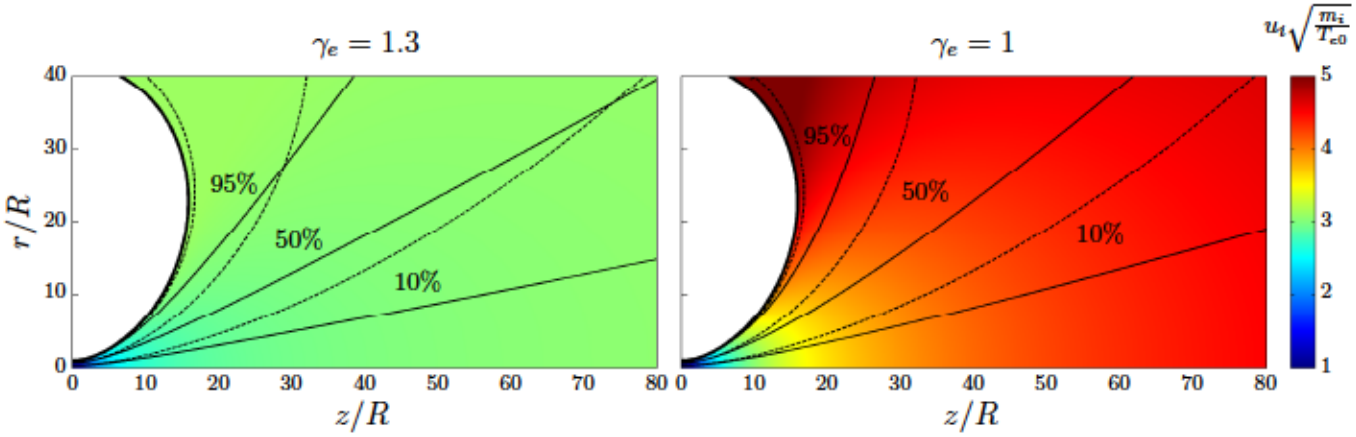

Fig. 4. Plasma velocity $u_i\sqrt{m_i/T_{e0}}$ (background map) for $\gamma_e = 1.3$ (left) and $\gamma_e = 1$ (right), with the ion streamtubes (solid) and the corresponding magnetic/electron streamtubes (dashed). The labels on the tubes indicate the fraction of ion (and electron/magnetic) flux carried by each tube (i.e., the normalized flux integral from the axis to the tube). The tube containing 100% of the plasma flux is the plasma edge, R_V.

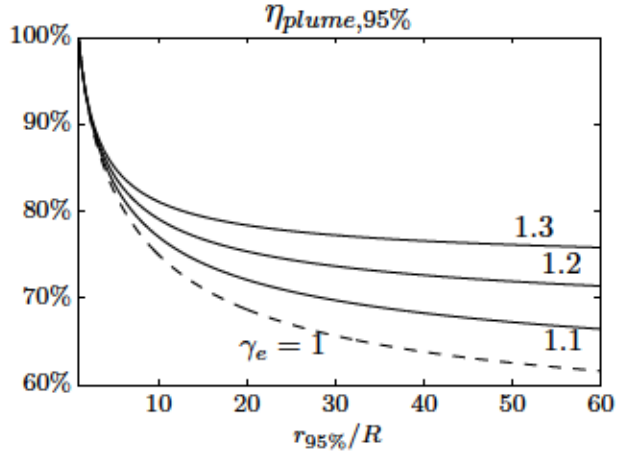

Fig. 5. Plume divergence efficiency $\eta_{plume,95\%}$ of the 95%-flux streamtube (defined in the text), for $\gamma_e = 1$ (dashed line) and 1.1, 1.2, 1.3 (solid lines). The efficiency is plotted against the radius of the 95%-flux tube, $r_{95\%}$.

by the ion 95%-flux ion tube at a $z = \text{const}$ section,

$$\eta_{plume,95\%}(z) = \frac{\int_0^{R_V(z)} rnu_{zi}^3 dr}{\int_0^{R_V(z)} rnu_i^2 u_{zi} dr}, \tag{13}$$

and is shown in Fig. 5 for different values of γ_e, plotted against the radius of the 95%-flux tube. Clearly, cooling plasmas yield a much higher efficiency downstream (about 15% more for $\gamma_e = 1.3$ than for $\gamma_e = 1$ at $r_{95\%} = 60R$), and $\eta_{plume,95\%}(z)$ decreases at a lower rate in the polytropic plasmas. While the present data does not allow us to infer an asymptotic limit for $\eta_{plume,95\%}(z)$, simple non-magnetized plasma plume models[41] show that isothermal plumes continue to diverge at a logarithmically-slow rate downstream due to the residual pressure, whereas polytropic plumes do have a final divergence angle.

Lastly, the existence of an asymptotic value of the electric potential helps to find a closure to the power balance in the plasma plume, required to compute the efficiency of a plasma thruster as a whole[9]. In essence, in the absence of dissipation, an electron expansion with $\gamma_e \neq 5/3$ (i.e., other than the adiabatic exponent) must be sustained by an electron heat flux $q_{\parallel e}$ coming from the plasma source that maintains a higher-than-adiabatic temperature in the plume; i.e., if the electrons cool down as $T_e \propto n^{\gamma_e - 1}$ instead of cooling down as $T_e \propto n^{2/3}$, the excess power needed to replenish their internal energy is provided by $-\partial q_{\parallel e}/\partial \mathbf{1}_\parallel$. Assuming that $q_{\parallel e}$ has to be enough to allow the plasma to expand down to $\phi = \phi_\infty$, we can estimate the electron heat flux at the MN throat from the integral energy equation applied between the throat and far downstream where the expansion can be considered complete. For the present simulations, this reads:

$$\begin{aligned} P_{beam} &= \dot{m}_i \left(\frac{u_{i0}^2}{2} + \frac{5}{2}\frac{T_{e0}}{m_i} \right) + Q_e(0) = \\ &= \dot{m}_i \left(\frac{u_{i0}^2}{2} + \frac{\gamma_e T_{e0}/m_i}{\gamma_e - 1} \right) \end{aligned} \tag{14}$$

where P_{beam} is the total power on any section of the jet, and $Q_e(z)$ is the integrated electron heat flux at section z. The total electron heat flux at the throat,

$$Q_e(0) = \frac{3}{2}\frac{\dot{m}_i T_{e0}}{m_i}\left(\frac{5/3 - \gamma_e}{\gamma_e - 1}\right), \tag{15}$$

has been plotted on Fig. 6 as a function of γ_e to show the strong influence of this parameter on the energy balance of the plume, specially near the isothermal limit (for which $Q_e(0) \to \infty$).

IV. Influence of Ion Thermal Energy

Both ion and electron thermal energy can be transformed into directed axial ion energy in the MN: in essence, the perpendicular energy of each charged particle is converted into parallel energy thanks to the inverse magnetic mirror effect. Notwithstanding, from a macroscopic point of view, the role of the thermal energy of each species is different. Electron thermal energy, on the one hand, causes electrons to expand and to create an ambipolar electric field that pulls ions downstream[10]. In this way, the internal electric field $-\nabla\phi$ acts as the intermediary for the plasma energy conversion. On the other hand, ion thermal energy is responsible for a

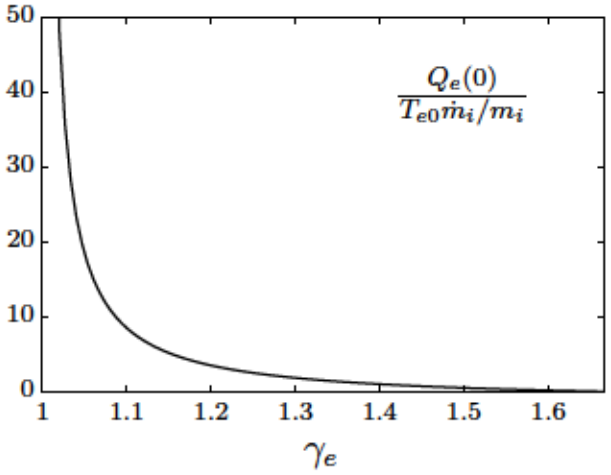

Fig. 6. Non-dimensional electron heat flux at the nozzle throat $Q_e(0)$ flowing out of the plasma source as a function of γ_e.

direct gasdynamic acceleration mechanism, which takes place without the mediation of any electric field, as stated by Eq. (3).

In an actual plasma thruster, thermal energy is divided between ions and electrons, although usually not evenly. This means that both acceleration mechanisms, ambipolar and gasdynamic, will coexist; the relevance of each of them depends on the fraction of thermal energy carried by each species, measured by the parameter T_{i0}/T_{e0}: in some devices like the HPT, $T_{i0}/T_{e0} \ll 1$, suggesting that ion temperature can be safely neglected on a first analysis. On the contrary, the operation of other thrusters under development, such as the VASIMR, which incorporates an ion cyclotron resonance heater to increase the energy of the plasma after ionization in the source, deposit most of the energy on the ions, which can reach values of $T_{i0}/T_{e0} = \mathcal{O}(1)$–$\mathcal{O}(10)$. Nonetheless, as can be seen in Eqs. (8)–(10), the resulting (total) ion acceleration and thrust production depend only on the combined barotropy function h.

Dominant ion thermal energy in the model poses several questions on how does the perpendicular confinement of that energy take place in the initial plasma column. This can be understood by analyzing the radial balances at the MN throat. In the case when all pressure is carried by hot electrons, it is effectively confined by the magnetic force on them: the gyration of each electron about its magnetic line adds up to give rise to the azimuthal diamagnetic drift, which sets up a radial force balance at the throat: $\partial p/\partial r \equiv -en u_{\theta e,dia m} B$. No initial radial electric field is required, as the $T_i = 0$ ions are already in radial equilibrium. The initial condition used in the simulations of the previous section are based on this force balance. In contrast, when ions carry part of the thermal energy, the extra radial pressure has to be confined too. This can be achieved, in principle, by an azimuthal ion drift $u_{\theta i,dia m}$, similar but opposite to the electron drift, or by a radial electric field. However, except for higher magnetic strengths, the heavier ions are unmagnetized at the throat, meaning that we cannot count on magnetic forces to balance the perpendicular expansion of the ion population. Indeed, the expected scenario in that case is that ions are confined by a radial electric field $-\partial\phi/\partial r = \partial p_i/\partial r$ set up by the electrons as the ions pull outward, while the ion azimuthal velocity remains negligibly low. This, in turn, increases the demand on electron azimuthal velocity, which must now confine themselves and the ions too, and an additional drift $u_{\theta e,E\times B} \equiv -(\partial\phi/\partial r)/B$ develops. The summation of both drifts, $u_{\theta e,dia m}$ and $u_{\theta e,E\times B}$, gives the total electron azimuthal velocity at the throat, $u_{\theta e}$, which can be concentrated at the plasma edge if the initial density profile is uniform[10], or distributed radially if it is non-uniform, as determined by Eq. (9).

Like at the throat section, ion pressure can affect strongly the shape of the confining ambipolar potential downstream. To illustrate this effect, Fig. 7 presents, for different values of T_{i0}/T_{e0}, the electric potential for the plasma jet with an initially non-uniform profile with $n = J_0(a_0 r/R)$ and $u_{\theta i} = 0$ (unmagnetized ions), where J_0 is the Bessel function of the first kind of order 0, and a_0 is its first zero. For simplicity, both ions and electrons have been considered isothermal here.

The first aspect that can be observed is a lower potential drop along the MN (normalized with the 'total' temperature $T = T_e + T_i$), as $\partial\phi/\partial \mathbf{1}_\parallel$ depends only on T_e (Eq. (8)). Hence, the parallel ambipolar electric field becomes weaker as the ions carry a larger fraction of the total thermal energy. Second, as it can be seen by the convexity of the isopotential lines in Fig. 7, the ambipolar electric potential decreases monotonically downstream and outward only when $T_{i0}/T_{e0} = 0$; in any other cases, $-\partial\phi/\partial r$ points inward initially, in the neighborhood of the throat, to confine the radial expansion of ions, and only later downstream $-\partial\phi/\partial r$ points outward again. This reflects the change in the character of the electric field within the plasma from electron-confining (and ion-expanding) to ion-confining as the ratio T_{i0}/T_{e0} is increased.

Finally, the cooling rates of ions and electrons (represented here by the effective values of γ_i and γ_e), need not be equal in the expansion, but can depend on the detailed kinetic behavior of each species. This adds another parameter to characterize the role of the two acceleration mechanisms in the MN. As an example of one of the possible cases, Fig. 8 depicts the relative importance of the ion gasdynamic acceleration mechanism on the expansion, as the accumulated increase of ion kinetic energy due to ion thermal energy, for $T_{i0}/T_{e0} = 5$, $\gamma_i = 5/3$ (adiabatic), $\gamma_e = 1$ (isothermal), and an initially uniform plasma profile with $n = n_0$ and $u_{\theta i} = 0$ at the throat. The remaining fraction of the acceleration is afforded by the ambipolar mechanism, sustained by electron thermal energy. Clearly, in this particular case, due to the different cooling rates of each species, the weight of the gasdynamic mechanism is largest near the MN throat, where T_i is high, accounting for nearly five sixths of the total acceleration. As the expansion proceeds, however, the ion population cools down faster than the electrons, and the gasdynamic mechanism loses importance in favor for the ambipolar one. This is observed as a lower fraction of the total acceleration caused by ion thermal energy downstream. Eventually, ions cool down and the residual acceleration is caused only by the ambipolar electric field set up by the electrons. The analysis of more complex cases with

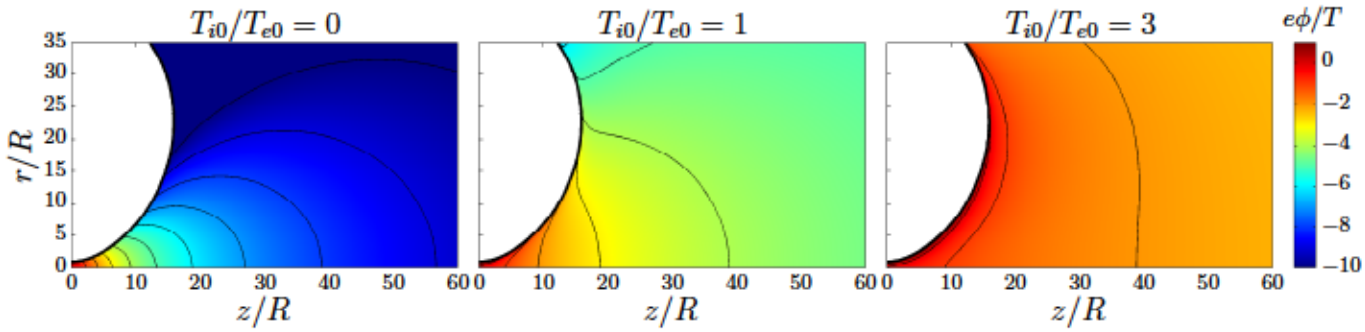

Fig. 7. Electric potential ϕ for $T_{i0}/T_{e0} = 0$, 1 and 3, for an initially non uniform plasma jet. The electric potential has been normalized with the 'total' temperature $T = T_e + T_i$. Solid lines represent isopotential surfaces in the plasma, spaced in increments of $e\Delta\phi/T = 1$.

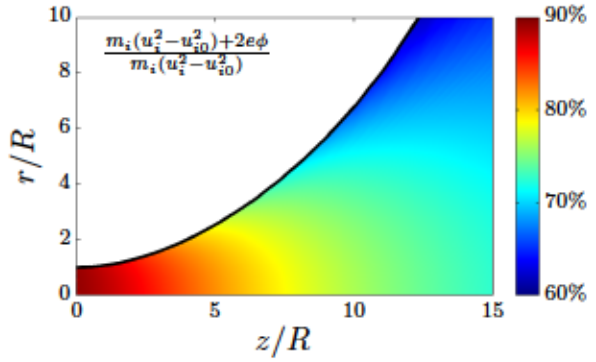

Fig. 8. Fraction of the total ion kinetic energy gain, $m_i(u_i^2 \quad u_{i0}^2)/2$, afforded by the ion thermal energy, giving rise to the direct gasdynamic acceleration mechanism.

other values of γ_e and γ_i is straightforward.

V. Conclusion

In the present paper we have extended our 2D plasma/MN model[10] to include simple, adjustable thermodynamic models for ions and electrons, as a first stage to understand the consequences of electron cooling and ion thermal energy on the expansion. The resulting model can be regarded as a simple, practical tool to explore the effects of different cooling rates on the operation of the magnetic nozzle.

Electron cooling, an expected feature of the flow due to the unsustainability of isothermality downstream[34], is seen to affect most of the phenomena of the far-region, including radial rarefaction and ion streamline separation. In particular, electron cooling is central in plasma detachment, with a higher cooling rate leading to earlier separation from the MN. In this regard, an isothermal model, albeit unphysical in some aspects, can be used to obtain a conservative limit for detachment. Cooling also plays a central role in the energy balance in the plasma plume, and thus in the production of thrust. As such, uncertainties in the effective electron cooling rate introduce large uncertainties on the steady-state expansion.

In regard to ions, inclusion of their thermal energy in the model allows to investigate the combined gasdynamic and ambipolar acceleration mechanisms. Again, the ability to include non-isotropic populations is deemed an important aspect, which will be object of future work. Non-isotropic distribution functions give rise to explicit magnetic mirror terms in the fluid equations, and a detailed model of the ion species is particularly relevant to high-ion-energy devices such as the VASIMR, where the ion energy is highly collimated as ion gyromotion. The structure of the electric field in the expansion, the confinement of the plasma thermal energy, and the radial balance of the plasma at the MN throat have been shown to depend on the fraction of the energy carried by ions in the low-ion-magnetization limit of interest for propulsion.

Further work must identify the exact mechanisms that enable a magnetized, collisionless electron population to cool down, and assess the heat fluxes along the magnetic field. Observe that the complexity of the thermodynamic behavior of electrons and ions in MN-based devices will demand advanced models, taking into account kinetic considerations. Work in this area has been initiated by Martínez-Sánchez and Navarro[42], following a similar approach as that in Ref. [43] for a convergent magnetic field geometry. A proper cooling model will also address the non-isotropization of the species downstream, the demagnetization of electrons, and allow for the inclusion of collisions within the plasma jet and with an ambient plasma. The bi-polytropic plasma model described here, while unable to reproduce these phenomena, can be regarded as a simplified tool to study the effects of cooling, once that the effective γ_e and γ_i are modeled or estimated by other means.

Acknowledgments

This work is sponsored by the Spanish R & D National Plan (Project AYA-2010-61699). The authors thank M. Martínez-Sánchez and J. Navarro-Cavallé for the insightful discussions on electron cooling mechanisms.

References

[1] O. Batishchev, "Minihelicon plasma thruster," *IEEE Transaction on Plasma Science*, vol. 37, pp. 1563–1571, 2009.

[2] C. Charles, R. Boswell, and M. Lieberman, "Xenon ion beam characterization in a helicon double layer thruster," *Applied Physics Letters*, vol. 89, p. 261503, 2006.

[3] D. Pavarin, F. Ferri, M. Manente, D. Curreli, Y. Guclu, D. Melazzi, D. Rondini, S. Suman, J. Carlsson, C. Bramanti, E. Ahedo, V. Lancellotti, K. Katsonis, and G. Markelov, "Design of 50W helicon plasma thruster," in *31th International Electric Propulsion Conference*, ser. IEPC 2009-205, 2009.

[4] J. C. Sercel, "Electron-cyclotron-resonance (ECR) plasma acceleration," in *AIAA 19th Fluid Dynamics, Plasma Dynamics and Lasers Conference*, 1987.

[5] G. Krülle, M. Auweter-Kurtz, and A. Sasoh, "Technology and application aspects of applied field magnetoplasmadynamic propulsion," *J. Propulsion and Power*, vol. 14, pp. 754–763, 1998.

[6] V. Tikhonov, S. Semenikhin, J. Brophy, and J. Polk, "Performance of 130kW MPD thruster with an external magnetic field and Li as a propellant," in *Proceedings of the 25 th International Electric Propulsion Conference*, 1997, pp. 728–733.

[7] H.-B. Tang, J. Cheng, C. Liu, and T. M. York, "Study of applied magnetic field magnetoplasmadynamic thrusters with particle-in-cell and monte carlo collision. II. investigation of acceleration mechanisms," *Physics of Plasmas*, vol. 19, p. 073108, 2012.

[8] F. Diaz, J. Squire, R. Bengtson, B. Breizman, F. Baity, and M. Carter, "The physics and engineering of the VASIMR engine," in *36th AIAA/ASME/SAE/ASEE Joint Propulsion Conference & Exhibit*, ser. AIAA 2000-3756, 2000.

[9] E. Ahedo and J. Navarro-Cavallé, "Helicon thruster plasma modeling: Two-dimensional fluid-dynamics and propulsive performances," *Physics of Plasmas*, vol. 20, p. 043512, 2013.

[10] E. Ahedo and M. Merino, "Two-dimensional supersonic plasma acceleration in a magnetic nozzle," *Physics of Plasmas*, vol. 17, p. 073501, 2010.

[11] R. Gerwin, G. Marklin, A. Sgro, and A. Glasser, "Characterization of plasma flow through magnetic nozzles," Los Alamos National Laboratory, Tech. Rep. AFSOR AL-TR-89-092, 1990.

[12] S. Andersen, V. Jensen, P. Nielsen, and N. D'Angelo, "Continuous supersonic plasma wind tunnel," *Phys. Fluids*, vol. 12, pp. 557–560, 1969.

[13] K. Kuriki and O. Okada, "Experimental study of a plasma flow in a magnetic nozzle," *Physics of Fluids*, vol. 13, p. 2262, 1970.

[14] T. M. York, B. A. Jacoby, and P. Mikellides, "Plasma flow processes within magnetic nozzle configurations," *Journal of Propulsion and Power*, vol. 8, no. 5, pp. 1023–1030, 1992.

[15] M. Inutake, A. Ando, K. Hattori, H. Tobari, and T. Yagai, "Characteristics of a supersonic plasma flow in a magnetic nozzle," *J. Plasma Fusion Res.*, vol. 78, pp. 1352–1360, 2002.

[16] H. Kosmahl, "three-dimensional plasma acceleration through axisymmetric diverging magnetic fields based on dipole moment approximation," Tech. Rep., NASA TN D-3782, 1967.

[17] D. Chubb, "Fully ionized quasi-one-dimensional magnetic nozzle flow," *AIAA Journal*, vol. 10, pp. 113–114, 1972.

[18] J. Sercel, "Simple model of plasma acceleration in a magnetic nozzle," in *21st International Electric Propulsion Conference*, vol. 1, 1990.

[19] P. Mikellides, P. Turchi, and N. Roderick, "Applied-field magnetoplasmadynamic thrusters, part 1: Numerical simulations using the MACH2 code," *Journal of Propulsion and Power*, vol. 16, no. 5, 2000.

[20] B. Roberson, R. Winglee, and J. Prager, "Enhanced diamagnetic perturbations and electric currents observed downstream of the high power helicon," *Physics of Plasmas*, vol. 18, p. 053505, 2011.

[21] K. Takahashi, T. Lafleur, C. Charles, P. Alexander, R. W. Boswell *et al.*, "Axial force imparted by a current-free magnetically expanding plasma," *Physics of Plasmas*, vol. 19, no. 8, p. 083509, 2012.

[22] W. Cox, C. Charles, R. Boswell, and R. Hawkins, "Spatial retarding field energy analyzer measurements downstream of a helicon double layer plasma," *Applied Physics Letters*, vol. 93, p. 071505, 2008.

[23] C. Deline, R. Bengtson, B. Breizman, M. Tushentsov, J. Jones, D. Chavers, C. Dobson, and B. Schuettpelz, "Plume detachment from a magnetic nozzle," *Physics of Plasmas*, vol. 16, p. 033502, 2009.

[24] K. Terasaka, S. Yoshimura, K. Ogiwara, M. Aramaki, and M. Tanaka, "Experimental studies on ion acceleration and stream line detachment in a diverging magnetic field," *Physics of plasmas*, vol. 17, p. 072106, 2010.

[25] J. P. Squire, C. S. Olsen, F. R. Chang-Díaz, L. D. Cassady, B. W. Longmier, M. G. Ballenger, M. D. Carter, T. W. Glover, and G. E. McCaskill, "VASIMR VX-200 operation at 200 kW and plume measurements: Future plans and an ISS EP test platform," in *32nd International Electric Propulsion Conference*, 2011.

[26] K. Takahashi, Y. Itoh, and T. Fujiwara, "Operation of a permanent-magnets-expanding plasma source connected to a large-volume diffusion chamber," *Journal of Physics D: Applied Physics*, vol. 44, p. 015204, 2011.

[27] R. Moses, R. Gerwin, and K. Schoenberg, "Resistive plasma detachment in nozzle based coaxial thrusters," in *Proceedings Ninth Symposium on Space Nuclear Power Systems, Albuquerque, New Mexico, 1992*, ser. AIP Conference Proceedings No. 246, 1992, pp. 1293–1303.

[28] E. B. Hooper, "Plasma detachment from a magnetic nozzle," *Journal of Propulsion and Power*, vol. 9, no. 5, pp. 757–763, 1993.

[29] A. Arefiev and B. Breizman, "Magnetohydrodynamic scenario of plasma detachment in a magnetic nozzle," *Physics of Plasmas*, vol. 12, p. 043504, 2005.

[30] E. Ahedo and M. Merino, "On plasma detachment in propulsive magnetic nozzles," *Physics of Plasmas*, vol. 18, p. 053504, 2011.

[31] ——, "Two-dimensional plasma expansion in a magnetic nozzle: separation due to electron inertia," *Physics of Plasmas*, vol. 19, p. 083501, 2012.

[32] M. Merino and E. Ahedo, "Magnetic nozzle far-field simulation," in 48^{th} *AIAA/ASME/SAE/ASEE Joint Propulsion Conference & Exhibit*, no. AIAA-2012-3843, 2012.

[33] M. A. Raadu, "Expansion of a plasma injected from an electrodeless gun along a magnetic field," *Plasma Physics*, vol. 21, no. 4, p. 331, 1979.

[34] A. Arefiev and B. Breizman, "Ambipolar acceleration of ions in a magnetic nozzle," *Physics of Plasmas*, vol. 15, p. 042109, 2008.

[35] ——, "Collisionless plasma expansion into vacuum: Two new twists on an old problem," *Physics of Plasmas*, vol. 16, p. 055707, 2009.

[36] B. Bezzerides, D. Forslund, and E. Lindman, "Existence of rarefaction shocks in a laser-plasma corona," *Phys Fluids*, vol. 21, pp. 2179–2186, 1978.

[37] E. Ahedo and M. Martínez-Sánchez, "Theory of a stationary current-free double layer in a collisionless plasma," *Physical Review Letters*, vol. 103, p. 135002, Sep 2009.

[38] M. Merino and E. Ahedo, "Two-dimensional quasi-double-layers in two-electron-temperature, current-free plasmas," *Physics of Plasmas*, vol. 20, p. 023502, 2013.

[39] C. Charles and R. Boswell, "Current-free double-layer formation in a high-density helicon discharge," *Applied Physics Letters*, vol. 82, p. 1356, 2003.

[40] M. Merino and E. Ahedo, "Plasma detachment mechanisms in a magnetic nozzle," in 47^{th} *AIAA/ASME/SAE/ASEE Joint Propulsion Conference & Exhibit*, no. AIAA-2011-5999. Washington DC: AIAA, 2011.

[41] M. Merino, E. Ahedo, C. Bombardelli, H. Urrutxua, and J. Peláez, "Hypersonic plasma plume expansion in space," in 32^{nd} *International Electric Propulsion Conference*, no. IEPC-2011-086. Fairview Park, OH: Electric Rocket Propulsion Society, 2011.

[42] M. Martínez-Sánchez and J. Navarro-Cavallé, private communication, 2013.

[43] M. Martínez-Sánchez and E. Ahedo, "Magnetic mirror effects on a collisionless plasma in a convergent geometry," *Physics of Plasmas*, vol. 18, 2011.

Mario Merino is a PhD Aerospace Engineer by Universidad Politécnica de Madrid, where he was teaching assistant for three years. Currently, Mario is an assistant professor at Universidad Carlos III de Madrid, actively researching on the modeling and simulation of plasma propulsion systems (in particular, magnetic nozzles and helicon plasma thrusters), space debris active removal systems, and plasma plume expansion into vacuum.

Eduardo Ahedo received MSc and PhD degrees in Aeronautical Engineering from the Universidad Politécnica de Madrid in 1982 and 1988, respectively. In 1989-90 he was a Fulbright postdoctoral scholar at the Massachusetts Institute of Technology. Currently, he is Professor of Aerospace Engineering at the Universidad Carlos III de Madrid. His research background covers modeling and simulation in plasma propulsion, plasma confinement, plasma instabilities, electrodynamic tethers, plasma contactors, and plasma-laser interaction.